JCTC Journal of Chemical Theory and Computation

Fisher Information Study in Position and Momentum Spaces for Elementary Chemical Reactions

Sheila López-Rosa,[†,‡] Rodolfo O. Esquivel,*[,‡,§] Juan Carlos Angulo,[†,‡] Juan Antolín,[‡,||] Jesús S. Dehesa,[†,‡] and Nelson Flores-Gallegos[§]

Departamento de Física Atómica, Molecular y Nuclear, Universidad de Granada, 18071-Granada, Spain, Instituto Carlos I de Física Teórica y Computacional, Universidad de Granada, 18071-Granada, Spain, Departamento de Química, Universidad Autónoma Metropolitana, 09340-México D.F., México, and Departamento de Física Aplicada, EUITIZ, Universidad de Zaragoza, 50018-Zaragoza, Spain

Received October 15, 2009

Abstract: The utility of the Fisher information measure is analyzed to detect the transition state, the stationary points of a chemical reaction, and the bond breaking/forming regions of elementary reactions such as the simplest hydrogen abstraction and the identity S_N2 exchange ones. This is performed by following the intrinsic reaction path calculated at the MP2 and QCISD(T) levels of theory with a 6-311++G(3df, 2p) basis set. Selected descriptors of both position and momentum space densities are utilized to support the observations, such as the molecular electrostatic potential (MEP), the hardness, the dipole moment, along with geometrical parameters. Our results support the concept of a continuum of transient of Zewail and Polanyi for the transition state rather than a single state, which is also in agreement with reaction force analyses.

Introduction

Notwithstanding that Fisher information of a probability distribution was introduced in the 1920s,[1] its utility for the informational description of relevant physical and chemical systems and/or processes, such as atoms,[2,3] molecules,[4] ionization,[5] and reactions, among many others, has been assessed until recently. Its appealing features differ appreciably from other information measures because of its "local" character,[6] in contrast with the "global" nature of several functionals, such as the variance or the Shannon, Tsallis, and Renyi entropies.

The local character of Fisher information provokes an enhanced sensitivity to strong changes, even over a very small-sized region in the domain of definition, because of its definition as a functional of the distribution gradient, as will be described below. This is not the case for the global information measures (e.g., Shannon entropy, disequilibrium, variance),[7] whose values are conditioned by the behavior of the density over the whole domain and display much lower variations as a consequence of the strongly localized changes on its values.

Aside from the relevance of the Fisher information itself for the interpretation of different physical and chemical phenomena within an information-theoretical framework, mainly for one-particle densities in conjugated spaces for many-electron systems (e.g., atoms and molecules) and processes (e.g., ionization dissociation or reactions), among others, it is also a component of different complexity measures,[8] a concept that nowadays constitutes a hot topic for study as a tool for the informational analysis of the aforementioned systems and processes. Different complexities include in their definition the Fisher information as an essential ingredient to quantify the level of localization or organization for the considered distribution. Such is the case, for instance, of the recently introduced "Fisher−Shannon"[3] and "Cramer−Rao"[8] complexities, where information on randomness or uncertainty is provided, respectively, by the

* Corresponding author e-mail: esquivel@xanum.uam.mx.
† Departamento de Física Atómica, Universidad de Granada.
‡ Instituto Carlos I de Física Teórica y Computacional, Universidad de Granada.
§ Universidad Autónoma Metropolitana.
|| Universidad de Zaragoza.

10.1021/ct900544m
Published on Web 12/22/2009

Shannon entropy and the variance. Exhaustive recent studies of these complexities for atomic systems can be found in ref 9.

Moreover, the concept of Fisher information for a given distribution has given rise to the introduction of information functionals with the aim of establishing a comparative measure between two different densities retaining the aforementioned local character of the quantifier for performing such a comparison. Such is the case of the initially defined "relative Fisher information",[10] following a procedure similar to that done in the Shannon case for defining the so-called "Kullback−Leibler" relative entropy,[11] and later by symmetrizing the relative Fisher information, with the aim of being interpreted as a distance between distributions, resulting in a measure known as "Fisher Divergence",[12] in a similar way as the "Jensen−Shannon Divergence"[13] arises from the Shannon entropy. Most applications of the Fisher Divergence regard the comparison of a relevant density describing a given system with an a priori one, usually chosen according to a simplified model or by considering specifically known properties of the system under study, by imposing them on the reference or a priori one.

Theoretical chemistry has witnessed a great deal of research to study the energetics of chemical reactions.[14] For instance, a variety of calculations of potential energy surfaces have been performed at various levels of sophistication.[15] Within the broad scope of these investigations, particular interest has been focused on extracting information about the stationary points of the energy surface. Despite the fact that minima, maxima, and saddle points are useful mathematical features of the energy surface to reaction-path following,[16] it has been difficult to attribute too much chemical or physical meaning to these critical points.[17] Whereas the reaction rate and the reaction barrier are chemical concepts, which have been rigorously defined and experimentally studied since the early days of the transition state (TS) theory,[18] the structure of the TS remains as a quest of physical organic chemistry. Understanding the TS is a fundamental goal of chemical reactivity theories, which implies the knowledge of the chemical events that take place to better understand the kinetics and the dynamics of a reaction. On the other hand, a variety of density descriptors have been employed to study chemical reactions.[18,19] Among them, it is worthy to mention the reaction force studies on the potential energy of reactions, which have been employed to characterize changes in the structural and/or electronic properties in chemical reactions.[20,21] However, to the best of our knowledge, none of them has been able to conceptually describe the reaction mechanism of elementary reactions in a simple and direct fashion.

In past years, there has been an increasing interest to analyze the electronic structure of atoms and molecules by applying information theory (IT).[22] These works have shown that information-theoretic measures are capable of providing simple pictorial chemical descriptions of atoms and molecules and the processes they exert through the localized/delocalized behavior of the electron densities in position and momentum spaces. In a recent study,[23] we have provided evidence that supports the utility of the information-theoretic measures in position and momentum spaces to detect the transition state and the stationary points of elementary chemical reactions so as to reveal the bond breaking/forming regions of the simplest hydrogen abstraction and the identity of S_N2 exchange chemical processes.

To the best of our knowledge, no studies have been reported on the application of Fisher information on chemical reactions. The goal of the present study is to follow the IRC (internal reaction coordinate) path of some selected elementary chemical reactions to analyze the course of the reactions by use of the Fisher information in position and momentum spaces as well as other charge density descriptors such as the molecular electrostatic potential (MEP) along with some reactivity parameters of DFT, the hardness "η", and softness "S", so as to witness the density changes exerted by the molecular structures during the chemical process. Two elemental reactions were chosen: the chemical probes under study are the simplest hydrogen abstraction reaction $H^{\bullet} + H_2 \rightarrow H_2 + H^{\bullet}$ and the identity S_N2 reaction $H^- + CH_4 \rightarrow CH_4 + H^-$.

Theoretical Details

The central quantities under study are the Fisher information

$$I_r = \int \frac{|\vec{\nabla}\rho(\vec{r})|^2}{\rho(\vec{r})} \mathrm{d}^3 r \tag{1}$$

in position space and

$$I_p = \int \frac{|\vec{\nabla}\gamma(\vec{p})|^2}{\gamma(\vec{p})} \mathrm{d}^3 p \tag{2}$$

in momentum space, where $\rho(\vec{r})$ and $\gamma(\vec{p})$ denote the normalize-to-unity electron density distributions in the position and momentum spaces, respectively. The total electron density of a molecule, in the independent particle approximation, consists of a sum of contributions from electrons in occupied orbitals. Thus, in momentum space, the contribution from an electron in a molecular orbital $\varphi_i(\vec{p})$ to the total electron density is given by $|\varphi_i(\vec{p})|^2$. The orbitals $\varphi_i(\vec{p})$ are then related by Fourier transforms to the corresponding orbitals in position space $\phi_i(\vec{r})$. Standard procedures for the Fourier transformation of position space orbitals generated by ab initio methods have been described.[24] The orbitals employed in ab initio methods are linear combinations of atomic basis functions, and because analytic expressions are known for the Fourier transforms of such basis fuctions,[25] the transformations of the total molecular electronic wave function from position to momentum space are computationally straightforward.[26]

The position Fisher information, which is closely connected to the kinetic energy,[27] is a spreading measure of the electron density all over the space with a locality property because it is a function of its gradient. In contrast with the Shannon entropy (which is a global spreading measure), it measures the spatial pointwise concentration of the electronic probability cloud and quantifies the gradient content of the electron distribution, so revealing the irregularities of the density and providing a quantitative estimation of its (strong) oscillatory character. Next, it is very sensitive to the

electronic fluctuations so that it allows us to explore the changes of the electronic distributions in an accurate manner. A similar interpretation follows for the momentum Fisher information. Moreover, the position and momentum Fisher information are reciprocal measures that satisfy the uncertainty relation $I_r I_p \geq 4D^2$ for D-dimensional quantum systems.[28] So, for three-dimensional systems, they fulfill the inequality $I_r I_p \geq 36$.

In recent studies, we have assessed the utility of employing other chemical descriptors to interpret information-theoretic measures. In this study, we find it interesting to use the MEP, the hardness, geometrical parameters, dipole moment, and vibrational frequencies.

The MEP represents the molecular potential energy of a proton at a particular location near a molecule,[29] say at nucleus A. The electrostatic potential, V_A, is then defined as

$$V_A = \left(\frac{\partial E^{\text{molecule}}}{\partial Z_A}\right)_{N,Z_{B\neq A}} = \sum_{B\neq A} \frac{Z_B}{|R_B - R_A|} - \int \frac{\rho(\vec{r})\, d\vec{r}}{|\vec{r} - R_A|} \quad (3)$$

where $\rho(\vec{r})$ is the molecular electron density and Z_A is the charge on nucleus A, located at R_A. Generally speaking, negative electrostatic potential corresponds to an attraction of the proton by the concentrated electron density in the molecules from lone pairs, π-bonds, etc. (colored in shades of red in contour diagrams). Positive electrostatic potential corresponds to a repulsion of the proton by the atomic nuclei in regions where low electron density exists and the nuclear charge is incompletely shielded (colored in shades of blue in contour diagrams).

We have also evaluated some reactivity parameters that may be useful to analyze the chemical reactivity of the processes. Parr and Pearson proposed a quantitative definition of hardness (η) within conceptual DFT:[30]

$$\eta = \frac{1}{2S} = \frac{1}{2}\left(\frac{\partial \mu}{\partial N}\right)_{v(\vec{r})} \text{ where } \mu = \left(\frac{\partial E}{\partial N}\right)_{v(\vec{r})} \quad (4)$$

is the electronic chemical potential of an N electron system in the presence of an external potential $v(\vec{r})$, E is the total energy, and "S" is called the softness. Using finite difference approximation, eq 4 would be

$$\eta = \frac{1}{2S} \equiv (E_{N+1} - 2E_N + E_{N-1})/2 = (I - A)/2 \quad (5)$$

where E_N, E_{N-1}, and E_{N+1} are the energies of the neutral, cationic, and anionic systems; and I and A are the ionization potential (IP) and electron affinity (EA), respectively. Applying Koopmans' theorem,[31] eq 4 can be written as:

$$\eta = \frac{1}{2S} \equiv \frac{\varepsilon_{\text{LUMO}} - \varepsilon_{\text{HOMO}}}{2} \quad (6)$$

where ε denotes the frontier molecular orbital energies. In general terms, hardness and softness are good descriptors of chemical reactivity; the former measures the global stability of the molecule (larger values of η means less reactive molecules), whereas the S index quantifies the polarizability of the molecule.[32] Thus, soft molecules are more polarizable and possess predisposition to acquire additional electronic charge.[33] The chemical hardness "η" is a central quantity for use in the study of reactivity and stability, through the hard and soft acids and bases principle.[34]

Results and Discussion

The electronic structure calculations performed in this study were carried out with the Gaussian 03 suite of programs.[35] Reported TS geometrical parameters for the abstraction,[36] and the S_N2 exchange,[37] reactions were employed. Calculations for the IRC were performed at the MP2 (UMP2 for the abstraction reaction) level of theory with at least 35 points for each one of the directions (forward/reverse) of the IRC. Next, a high level of theory and a well-balanced basis set (diffuse and polarized orbitals) were chosen for determining all of the properties for the chemical structures corresponding to the IRC. Thus, the QCISD(T) method was employed in addition to the 6-311++G** basis set, unless otherwise stated. The hardness and softness chemical parameters were calculated by use of eqs 5 and 6 and the standard hybrid B*3*LYP (UB3LYP for the abstraction reaction) functional.[35] Molecular frequencies corresponding to the normal modes of vibration depend on the roots of the eigenvalues of the Hessian (its matrix elements are associated with force constants) at the nuclei positions of the stationary points. We have found it illustrative to calculate these values for the normal mode associated with the TS (possessing one imaginary frequency or negative force constant), which were determined analytically for all points of the IRC path at the MP2 (UMP2 for the abstraction reaction) level of theory.[35] The molecular Fisher information in position and momentum spaces for the IRC was obtained in this study by employing software developed in our laboratory along with 3D numerical integration routines[38] and the DGRID suite of programs.[26] The bond breaking/forming regions along with electrophilic/nucleophilic atomic regions were calculated through the MEP by use of MOLDEN.[39] Atomic units are employed throughout the study except for the dipole moment (debye), vibration frequencies (cm^{-1}), and geometrical parameters (angstroms).

Abstraction Reaction. The reaction $H_a^{\bullet} + H_2 \rightarrow H_2 + H_b^{\bullet}$ is the simplest radical abstraction reaction involving a free radical (atomic hydrogen) as a reactive intermediate. This kind of reaction involves at least two steps (S_N1 reaction type): in the first step, a new radical (atomic hydrogen in this case) is created by homolysis, and in the second one the new radical recombines with another radical species. Such homolytic bond cleavage occurs when the bond involved is not polar and there is no electrophile or nucleophile at hand to promote heterolytic patterns. When the bond is made, the product has a lower energy than the reactants, and it follows that breaking the bond requires energy.

Our calculations for this reaction were performed at two different levels: the IRC was obtained at the UMP2/6-311G level, and all properties at the IRC were obtained at the QCISD(T)/6-311++G** level of theory. As a result of the IRC, 72 points evenly distributed between the forward and

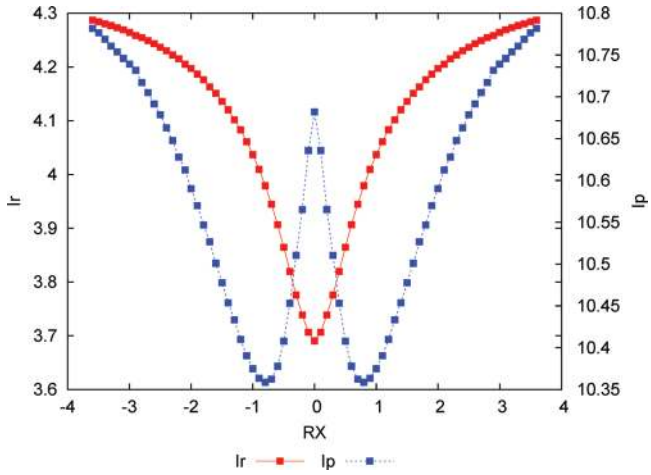

Figure 1. Fisher entropies in position (red line) and momentum (blue line) spaces for the IRC of $H_a^{\bullet} + H_2 \rightarrow H_2 + H_b^{\bullet}$.

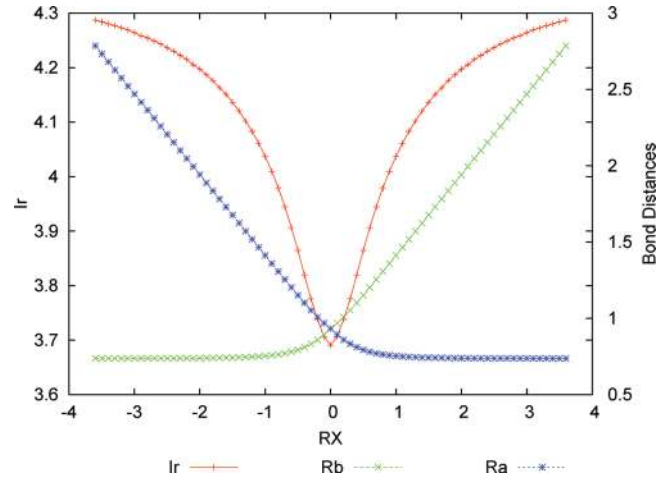

Figure 2. Fisher information in momentum space (red line) and the bond distances $R_a \equiv R(H_a{-}H)$ (blue line for the entering hydrogen) and $R_b \equiv R(H{-}H_b)$ (green line for the leaving hydrogen) for the IRC of $H_a^{\bullet} + H_2 \rightarrow H_2 + H_b^{\bullet}$.

reverse directions of the IRC were obtained. A relative tolerance of 1.0×10^{-5} was set for the numerical integrations.[38]

In Figure 1 is depicted the Fisher information in both position and momentum spaces. At a first glance, we observe that both quantities behave in a similar way toward the reactive complexes ($H_a^{\bullet}\cdots H{-}H$ and $H{-}H\cdots H_b^{\bullet}$) and tend to decrease toward the TS region, but with a very important difference that we analyze below. It is worth mentioning that, according to a previous study,[23] we have insight into the structural features of the distributions in both spaces, that is, concerning the spreading (localization/delocalization) of the densities. However, the behavior of the densities about their local changes (uniformity/irregularity) can only be provided by a local measure such as the Fisher information.

Both position and momentum Fisher information measures possess more structure at the vicinity of the TS as it may be observed from Figure 1. It is worthy to remark that this phenomenon is not present in the energy profile. By closer inspection, we note that the Fisher information I_r possesses a global minima at the TS, whereas the momentum one, I_p, possesses a local maxima and two local minimum at the vicinity of the TS (approximately $R_X \simeq 0.9$). This is interesting on chemical grounds because the structure observed for the Fisher information in momentum space at the vicinity of the TS can be associated with a process of bond breaking/forming (depending on the reaction direction) followed by stabilization of the structure at the TS.[23]

The chemical picture proceeds in this way: as the intermediate radical (H_a) approaches the molecule at the TS region, the molecular density exerts important changes so as to undergo the homolysis. This represents a physical situation where the density in position space gets localized in preparation for the bond rupture, which in turn results in a local increase of the kinetic energy. This provides explanation for the well-known fact that bond breaking requires energy. Next, the bond is formed, and, as a consequence, the TS structure shows lower kinetic energy than the reactant/product complex (H_a or H_b). Interestingly, from an information-theoretical point of view, all of the above happens: both I_r and I_p decrease as the radical intermediate approaches the molecule at the TS region, which means that the gradient of the density distributions (in both spaces) becomes smaller; that is, these densities are less irregular and more uniform. For the position space the Fisher information reaches a minimum at the TS; that is, at this point the position space density is the most uniform and delocalized (structurally less distorted with low kinetic energy and null dipole moment, see below) among all other structures at the vicinity of the TS. In momentum space, the Fisher information shows minima at the vicinity of the TS ($R_X \simeq |0.9|$) corresponding to a delocalized and uniform momentum density. It is worth noting that it is at these minima where the processes of bond breaking/forming occur.[23] At the TS, the Fisher information, I_p, is maximum corresponding with the least uniform and the highest localized momentum density with respect to the structures in its neighborhood. It is interesting to mention that minima of the Fisher information in momentum space coincide with the BCER (bond cleavage energy reservoir) defined in ref 23, and hence they might be characterized by the Fisher measure in momentum space.

To better understand the shape of the Fisher information, in Figure 2 are plotted the bond distances between the entering/leaving hydrogen radicals and the central hydrogen atom. This clearly shows that in the vicinity of the TS a bond breaking/forming chemical situation is occurring because the $R_b \equiv R(H{-}H_b)$ is elongating at the right side of the TS and the $R_a \equiv R(H_a{-}H)$ is stretching at the left side of the TS. It is worth noting that the chemical process does not happen in a synchronous manner; that is, the homolytic bond breaking occurs first, and then the molecule stabilizes by forming the TS structure, which is clearly observed in Figure 2. As the incoming radical approaches the molecule, the bond breaks. Because the Fisher information represents the gradient of a probability distribution, it is natural to associate this with the change in the corresponding density. Therefore, from Figure 2, one can see that as the incoming hydrogen approaches, the bond enlarges in the region where the Fisher information in momentum space increases more rapidly. In contrast, the Fisher information in position space is not describing the bond breaking/forming process.

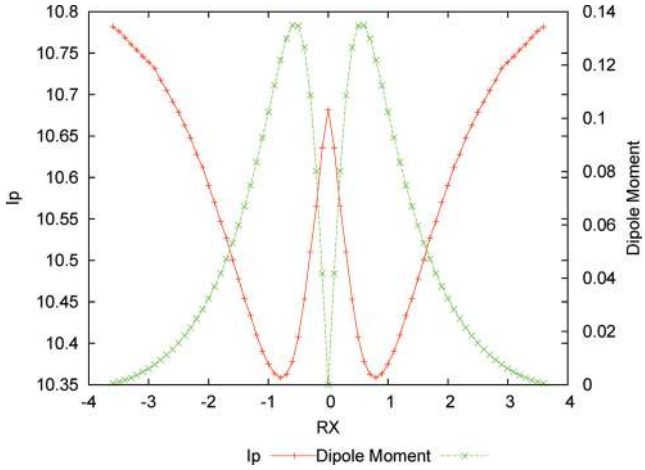

Figure 3. Fisher information in momentum space (red line) and the dipole moment values (green line) for the IRC of $H_a^{\bullet} + H_2 \rightarrow H_2 + H_b^{\bullet}$.

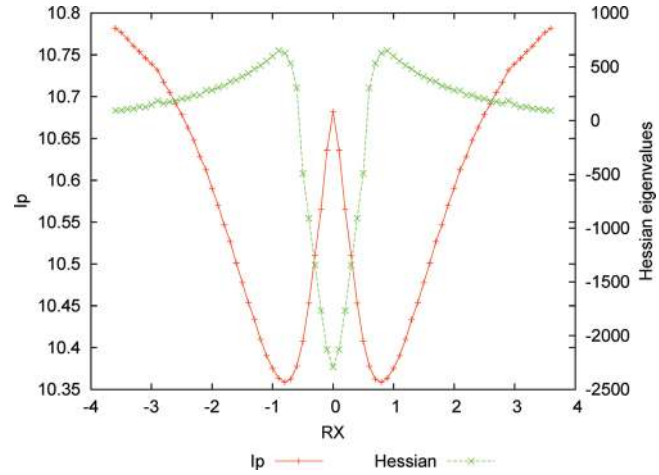

Figure 4. Fisher information in momentum space (red line) and the eigenvalues of the Hessian (green line) for the IRC of $H_a^{\bullet} + H_2 \rightarrow H_2 + H_b^{\bullet}$. It should be noted that negative values actually correspond with imaginary numbers (roots of negative force constants) so that the negative sign only represents a flag.

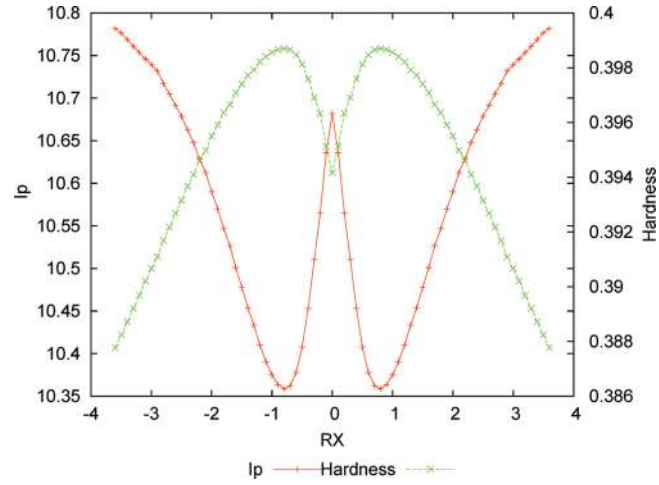

Figure 5. Fisher information in momentum space (red line) and the hardness values (green line) for the IRC of $H_a^{\bullet} + H_2 \rightarrow H_2 + H_b^{\bullet}$.

Next, we would like to test the nonpolar bond pattern characteristic of homolytic bond breaking reactions, which should be reflected through the dipole moment of the molecules at the IRC. This is indeed observed in Figure 3, where these values along with the ones of the momentum Fisher information are depicted for comparison purposes. At the TS the dipole moment is zero, and the same behavior is observed as the process tends to the reactants/products in the IRC, reflecting the nonpolar behavior of the molecule in these regions. However, it is also interesting to observe, from this property, how the molecular densities get distorted, reaching maximal values at the vicinity of the TS. In contrast, the behavior of the momentum Fisher information is totally opposite: this quantity decreases (increases) when the dipole moment increases (decreases), being minimum (maximum) approximately at the same points that the dipole moment reaches its maximum (minimum) value. It means that in the regions where the molecule has a nonpolar behavior, the momentum electronic density has a higher gradient content corresponding to a high irregular and localized density.

In Figure 4 are depicted the eigenvalues of the Hessian for the normal mode associated with the TS along the IRC of the reaction, along with the momentum Fisher information values. The Hessian values represent the transition vector "frequencies", which show maxima at the vicinity of the TS and a minimal value at the TS. Several features are worth mentioning: the TS corresponds indeed to a saddle point, and maxima at the Hessian correspond to high kinetic energy values (largest "frequencies" for the energy cleavage reservoirs correspond to the BCER[23]). In contrast, at the TS, the Hessian reaches a minimum value; this means that in this point the kinetic energy is the lowest one (minimal molecular frequency),[23] and, as we can see, it corresponds to a maximal Fisher information in momentum space. So it seems viable that I_p resembles the behavior of the TS vector. In connection with the Fisher information also depicted in Figure 4, it is interesting to note that in the transition state region (where the frequencies become imaginary[23,40]) the Fisher information exerts its largest change as a gradient of the distribution in momentum space.

There are several density descriptors used in chemistry to determine the reactivity behavior such as the hardness and softness (see the previous section). In Figure 5 we have plotted the values for the hardness along with the Fisher information in momentum space for comparison purposes. From a DFT conceptual point of view, we may interpret Figure 5 as that chemical structures at the maximal hardness (minimal softness) values possess low polarizability and hence are less prone to acquire additional charge (less reactive). These regions correspond to minimal Fisher information regions in momentum space associated with a highly uniform momentum density. According to considerations discussed above, these structures are found at the defined (in a previous work[23]) BCER regions; that is, they are maximally distorted, with highly delocalized momentum densities (maximal dipole moment values; see Figure 3). In contrast, hardness values are minimal at the reactant complexes regions, which correspond with localized momentum densities[23] with null dipole moments, and hence they are

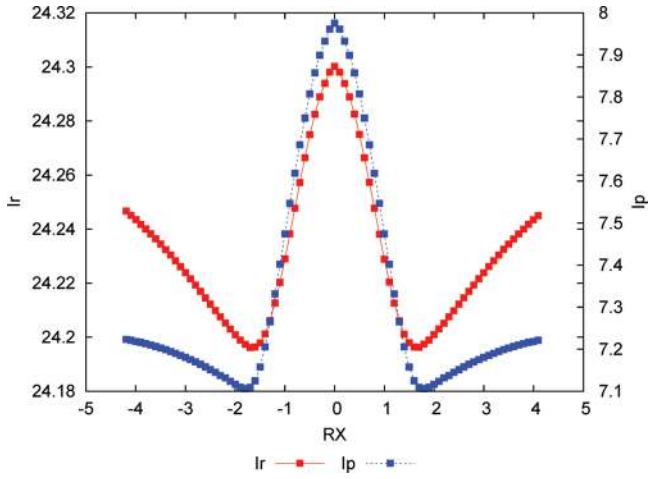

Figure 6. Fisher information in position (red line) and momentum (blue line) spaces for the IRC of $H_a^- + CH_4 \rightarrow CH_4 + H_b^-$.

more prone to react (more reactive). At the TS, a local minimum for the hardness may be observed; then it is locally more reactive and leaning to acquire charge because its dipole moment is null.

From the point of view of Fisher information, the TS represents a more irregular distribution. It is interesting to note that the I_r in Figure 1 can only be associated with the hardness at the TS (Figure 5), in that more reactive structures correspond to the most uniform density in position space.

Nucleophilic Substitution Reaction. In this part of the work, we analyze a typical nucleophilic substitution (S_N2) reaction whose chemical process involves only one step in contrast with the abstraction reaction studied before, which involves two steps. In the anionic form, the S_N2 mechanism can be depicted as

$$Y^- + RX \rightarrow RY + X^- \qquad (7)$$

which is characterized by being kinetically of second order (first order in each of the reactants: the nucleophile Y^- and the substrate R_X, where X^- is the nucleofuge or leaving atom). For identity S_N2 reactions, X = Y. It was postulated that the observed second-order kinetics is the result of passage through the well-known Walden inversion transition state where the nucleophile displaces the nucleofuge (leaving group) from the backside in a single concerted reaction step.

The $H_a^- + CH_4 \rightarrow CH_4 + H_b^-$ represents the typical identity S_N2 reaction, and we proceed with the calculations as follows: because diffuse functions are important to adequately represent anionic species,[20] we have performed calculations for the IRC at the MP2/6-311++G** level of theory, which generated 93 points evenly distributed between the forward and reverse directions of the IRC. Next, Fisher information in both position and momentum spaces and geometrical parameters at the IRC were calculated at the QCISD(T)/6-311++G** level of theory, which has been reported to be adequate for this kind of reaction.[41] A relative tolerance of 1.0×10^{-5} was set for the numerical integrations.[38]

If we represent both Fisher informations, I_r and I_p, in the same picture, Figure 6, we can observe that they show a similar structure, both possessing a maximum at the TS and minimal regions at its vicinity. This behavior is significantly different from the abstraction reaction analyzed before in that the position Fisher information shows the opposite behavior as compared to the momentum Fisher information at the TS region.

From a previous study[23] with Shannon entropies, we found a delocalized position density and a localized momentum density in the TS region, that is, corresponding with a chemically relaxed structure (structurally less distorted with low kinetic energy and null dipole moment, see below). In contrast, the reactive complexes toward reactants/products show more localized densities with less delocalized momentum densities; that is, the chemical structures at these regions are structurally distorted and possess more kinetic energy as compared to the TS. In the vicinity of the TS, at around $R_X \simeq |1.7|$, critical points for these measures are observed; they correspond to ionic complexes that characterize position densities, which are highly localized and with highly delocalized momentum densities and high kinetic energies. At a first glance, it seems likely that these regions correspond with BCER[23] where bond breaking may start occurring.

One of the principal differences between the S_N2 reaction with respect to the abstraction one is that for the former the course of the reaction occurs by an heterolytic rupture with an exchange of charge, whereas for the latter the mechanism is homolytic; that is, a spin coupling process occurs. In this reaction, as the incoming hydrogen approaches the molecule, it transfers charge, through the carbon bonding, to the leaving hydrogen so as to reach an equally charged distribution among the incoming/leaving hydrogens. As this process evolves, the gradient of the distribution involved in the position Fisher information I_r increases so as to reach a maximum at the TS.

To further support the charge transfer process mentioned above, we can witness the heterolytic bond/breaking process through the contour values of the MEP at several stages of the S_N2 reaction in the plane of the $[H_a \cdots C \cdots H_b]^-$ atoms. We may observe from Figure 7a the initial step of the bond breaking process for the leaving hydrogen (nucleofuge) at $R_X = -1.5$ (forward direction), by noting that this particular atom is losing bonding charge as it leaves (in the region where the potential is positive). This is in contrast with the entering hydrogen, which possesses the nucleophilic power of an hydride ion (in the region where the potential is negative). It is also interesting to note that the remaining attached hydrogen atoms possess the expected electrophilic nature of the molecular bonding environment, although its "philic" nature barely changes. In Figure 7b at $R_X = -0.9$ in the forward direction of the reaction, the $C-H_b$ bond cleavage is about to complete as the H_b atom has lost bonding charge (maximum electrophilic power) and the nucleophilic hydrogen is about to form a new bond by losing charge (nucleophilic power). In Figure 7c, we have depicted the MEP at the TS where we can observe the point where the gradient of the position density reaches its maximum due to the charge becoming equalized according to Figure 6.

To analyze in detail this reaction, we find it instructive to plot the distances between the nucleophilic hydrogen (H_a)

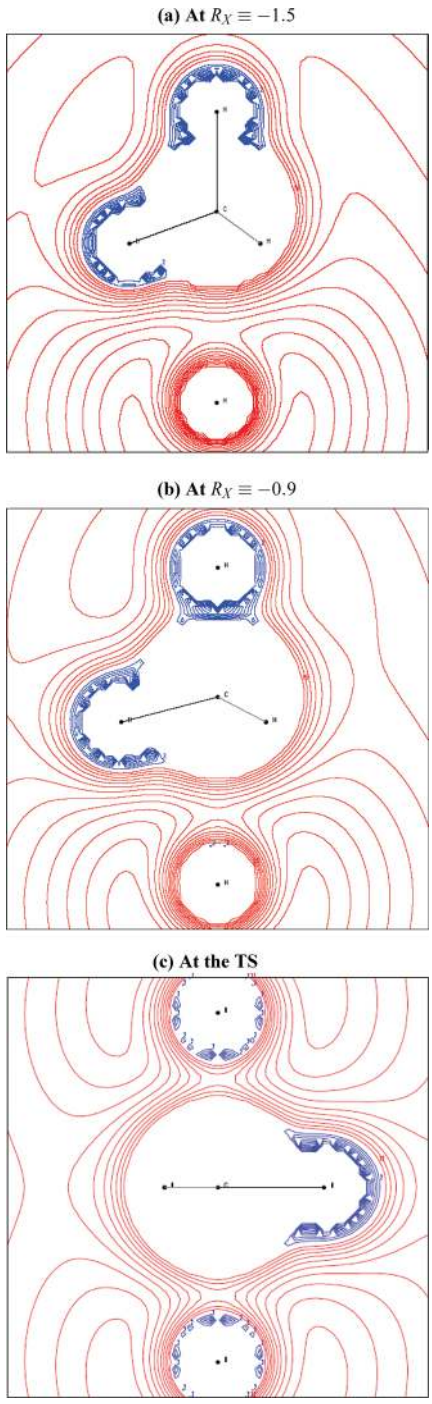

Figure 7. The MEP contour lines in the plane of $[H_a \cdots C \cdots H_b]^-$ (H_a stands for the nucleophilic atom and H_b is the nucleofuge, on bottom and top, respectively) showing nucleophilic regions (blue contour lines) and electrophilic regions (red contour lines) at several reaction coordinates for the S_N2 reaction at (a) $R_X = -1.5$, (b) $R_X = -0.9$, and (c) the TS.

and the leaving hydrogen (H_b) in Figure 8. Distances show the stretching/elongating features associated with the bond forming/breaking situation that we have anticipated before. In contrast with the previous analyzed abstraction reaction, the S_N2 reaction occurs in a concerted and synchronous manner; that is, the bond breaking/forming occurs at unison. An interesting feature that might be observed from Figure 8 is that, whereas the elongation of the carbon−nucleofuge

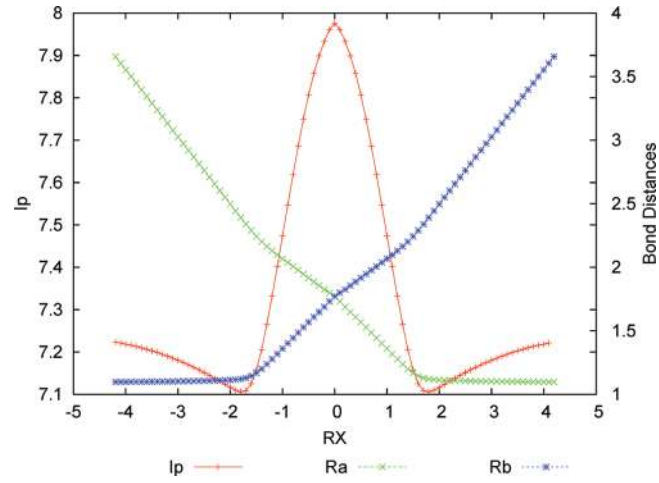

Figure 8. Fisher entropy in momentum space (red line) and the bond distances $R_a \equiv R(H_a{-}C)$ (green line, where H_a stands for the nucleophile) and $R_b \equiv R(C{-}H_b)$ (blue line, where H_b stands for the nucleofuge) for the IRC of $H_a^- + CH_4 \rightarrow CH_4 + H_b^-$.

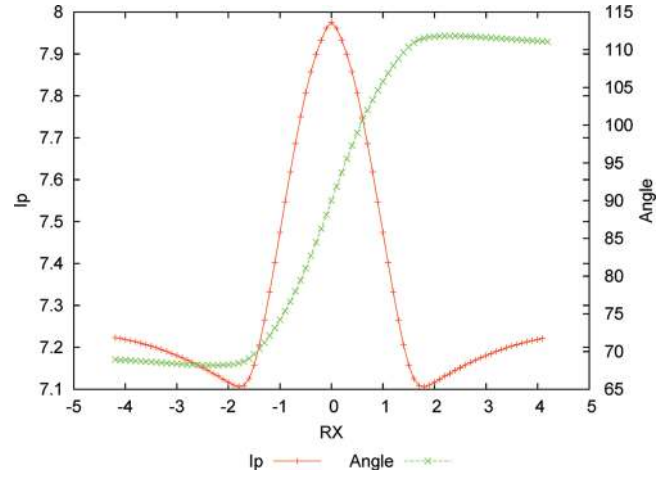

Figure 9. Fisher information in momentum space (red line) and the internal angle $H_a^- \cdots C{-}H$ (green line, where H_a stands for the nucleophile and H stands for any hydrogen attached to the methyl molecule) in degrees for the IRC of $H_a^- + CH_4 \rightarrow CH_4 + H_b^-$.

bond (R_b) changes its curvature significantly at $R_X \simeq -1.7$ (forward direction of the reaction), the stretching of the nucleophile−carbon bond does it in a smooth way, due to the repulsive forces that the ionic molecule exerts as the nucleophile approaches, which provokes the breaking of the carbon−nucleofuge to happen as the molecule starts liberating its kinetic energy. In this sense is that the reaction occurs in a concerted manner; that is, the bond breaking/dissipating energy processes occur simultaneously. It is interesting to note that minima for the momentum Fisher information coincide with the bond breaking/forming regions and that the change in the curvature of the bond distances marks the region where the gradient of the density in momentum space starts increasing.

In Figure 9, we have plotted the internal angle between $H_a^- \cdots C{-}H$ along with the Fisher information in momentum space for comparison purposes. Thus, the internal angle shows clearly that the molecule starts exerting the so-called

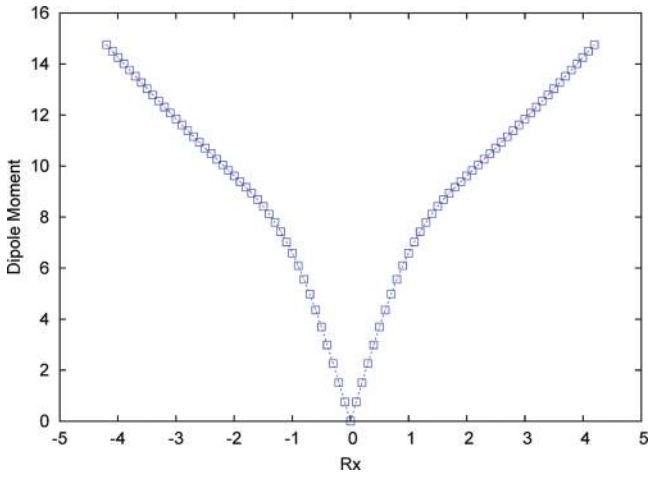

Figure 10. Dipole moment for the IRC of $H_a^- + CH_4 \rightarrow CH_4 + H_b^-$.

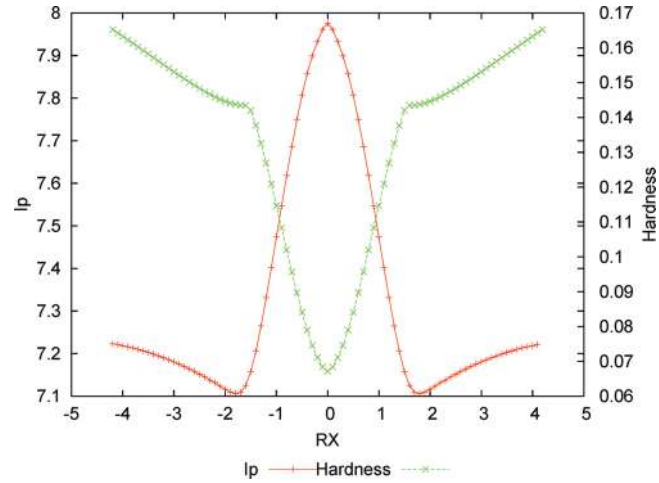

Figure 11. Fisher information in momentum space (red line) and the hardness values (green line) for the IRC of $H_a^- + CH_4 \rightarrow CH_4 + H_b^-$.

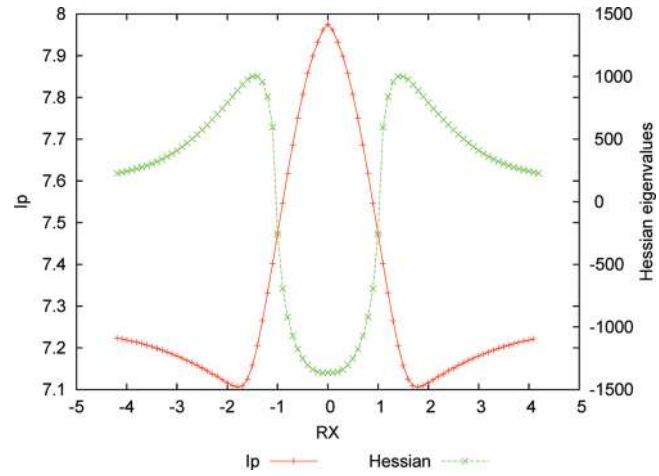

Figure 12. Fisher entropy in momentum space (red line) and the Hessian eigenvalues (green line) for the IRC of $H_a^- + CH_4 \rightarrow CH_4 + H_b^-$. It should be noted that negative values actually correspond with imaginary numbers (roots of negative force constants) so that the negative sign only represents a flag.

"inversion of configuration" at around $R_X \simeq -1.7$, where the nucleophile starts displacing the nucleofuge from the backside of the molecule in a single concerted reaction step. This starts occurring at the BCER regions.[23] We may observe from the figure that I_p possesses two minimum values that coincide with the inflection points of the angle, so marking the regions where the inversion of configuration occurs, that is, the region where the gradient increases and the momentum density distribution becomes less irregular.

The S_N2 reaction is a good probe to test the polar bond pattern characteristic of heterolytic bond breaking (with residual ionic attraction because of the ionic nature of the products), which should be reflected through the dipole moment of the molecules at the IRC. This is indeed observed in Figure 10, where these values along with the ones of the Fisher momentum information are depicted for comparison purposes. At the TS, the dipole moment is zero, showing the nonpolar character of the TS structure with both nucleophile/nucleofuge atoms repelling each other evenly through its carbon bonding. As the ionic complexes approach the reactants/products regions, the dipole moment increases monotonically, reflecting the polar bonding character of these ionic molecules with a significant change of curvature at the TS vicinity at around $R_X \simeq |1.0|$ (a change of curvature was already noted for Fisher information in momentum space at the same region). In going from reactants to products, it is evident that the inversion of the dipole moment values reflects clearly the inversion of configuration of the molecule (this reaction starts and ends with a tetrahedral sp^3 carbon in the methyl molecule passing through a trigonal bipyramid at the TS), which is an inherent feature of S_N2 reactions. At these regions, the gradient increases up to a maximum at the TS.

We found it illustrative to include the hardness values of the IRC in the analysis, which is depicted in Figure 11. We can observe that the hardness shows largest values toward the reactant/product regions and minima at the TS, where the Fisher information in momentum space gets a maximum value. The TS corresponds with a metastable structure with a lowest hardness (largest softness); that is, it is the most polarizable structure as compared to the rest at the IRC, and hence it is the most reactive. Also, it may be observed that the reactive complexes toward the reactant/product regions possess the largest hardness (lowest softness), which corresponds to highly stable molecules that are less prone to acquire additional charge. In the vicinity of the TS, we find "hardness bassins" at the BCER that we interpret to be chemically metastable and energetically reactive regions. We note from Figure 11 that the momentum Fisher information reflects the behavior above-described as an increment of the gradient.

The eigenvalues of the Hessian for the normal mode associated with the TS along the IRC of the reaction are depicted in Figure 12 along with the Fisher information values in momentum space. As it may be observed from this figure, the Hessian values show maxima at the BCER and reach its minimal value at the TS. The former are associated with high kinetic energy values (high vibrational frequencies), which seem to coincide with the minimal values in the momentum Fisher information profile. The TS at the saddle point is associated with a low kinetic energy structure

at the minimal molecular frequency value of the Hessian profile and with a maximum value of the Fisher information in momentum space, which corresponds to a density with the highest gradient content (very irregular density). It is important to mention that in the region where the frequencies become imaginary a transient of continuum has been established by Zewail and Polanyi[42] for the transition region, and this is clearly reflected by the zone where the gradient increases in momentum space and, consequently, the associated Fisher information increases too.

Conclusions

In this work, we have shown the usefulness of the information-theoretic measures of the Fisher type to characterize elementary chemical reactions. In a previous work,[23] the Shannon entropy of elementary chemical reactions was studied as a global measure that quantifies the localization/delocalization of the density; however, the behavior of the densities about their local changes (uniformity/irregularity) can only be provided by a local measure such as the Fisher information. In the previous sections, we have verified that the local character of Fisher information indeed provokes an enhanced sensitivity to changes on the position and momentum densities along the chemical reaction paths. One of the manifestations of the local changes excerted by the densities is due to the charge transfer process, which is directly reflected in the heterolitic behavior of the S_N2 reaction in contrast with the abstraction reaction whose mechanims are homolitic; that is, the Fisher information is capable of differentiating between both types of mechanims because of its local character.

The TS structure, at least for the studied reactions in this work, was clearly predicted by Fisher information in both spaces, whereas the stationary points that delimit the TS region are predicted by the momentum Fisher information solely. Besides, through the chemical probes we were capable of observing the basic chemical phenomena of bond breaking/forming showing that the Fisher information measures are highly sensitive in detecting these chemical events, mainly in momentum space.

It is interesting to mention that the uncertainty relation $I_r I_p \geq 36$, recently pointed out[28] for three-dimensional quantum systems, has been corroborated for the atomic and molecular systems involved in this study, which is a further check of our results.

According to Fisher information in position space, it is possible to detect differences in the mechanism for both reactions in that for the S_N2 the measure is able to witness the charge exchange process where the Fisher information is maximum at the TS. It remains to be studied whether the overall behavior of the abstraction reaction as compared to the exchange S_N2 reactions represents a manner of studying reaction mechanisms for Fisher information measures. We are aware of the fact that more chemical probes are necessary to pose more general statements.

Acknowledgment. We wish to thank José María Pérez-Jordá and Miroslav Kohout for kindly providing their numerical codes. R.O.E. wishes to thank Juan Carlos Angulo and Jesús Sánchez-Dehesa for their kind hospitality during his sabbatical stay on the Departamento de Física Atómica, Molecular y Nuclear and the Instituto Carlos I de Física Teórica y Computacional at the Universidad de Granada, Spain. We acknowledge financial support through Mexican grants 08226 CONACyT, PIFI 3.3 PROMEP-SEP and Spanish grants MICINN projects FIS-2008-02380, FIS-2005-06237 (J.A.), FQM-1735, and P06-FQM-2445 of Junta de Andalucía. J.A., J.C.A., J.S.D., and S.L.-R. belong to the Andalusian research group FQM-0207. Allocation of supercomputing time from the Departamento de Supercómputo at DGSCA-UNAM, the Sección de Supercomputacion at CSIRC-Universidad de Granada, and the Laboratorio de Supercómputo y Visualización at UAM is gratefully acknowledged.

References

(1) Fisher, R. A. *Proc. Cambridge Philos. Soc.* **1925**, *22*, 700.

(2) González-Férez, R.; Dehesa, J. S. *Eur. J. Phys. D* **2005**, *32*, 39.

(3) Angulo, J. C.; Antolín, J.; Sen, K. D. *Phys. Lett. A* **2008**, *372*, 670.

(4) Nalewajski, R. F. *Information Theory of Molecular Systems*; Elsevier Science: New York, 2006.

(5) Sen, K. D.; Panos, C. P.; Chatzisavvas, K. Ch.; Moustakidis, Ch. C. *Phys. Lett. A* **2007**, *368*, 286.

(6) Frieden, B. R. *Science from Fisher Information*; Cambridge University Press: New York, 2004.

(7) Cover, T. M.; Thomas, J. A. *Elements of Information Theory*; Wiley-Interscience: New York, 1991.

(8) Angulo, J. C.; Antolín, J. *J. Chem. Phys.* **2008**, *128*, 164109.

(9) Panos, C. P.; Chatzisavvas, K. C.; Moustakidis, C. C.; Kyrkou, E. *Phys Lett. A* **2007**, *363*, 78. Borgoo, A.; de Proft, F.; Geerlings, P.; Sen, K. D. *Chem. Phys. Lett.* **2007**, *444*, 183. Antolin, J.; Angulo, J. C. *Int. J. Quantum Chem.* **2009**, *109*, 586.

(10) Taneja, I. J.; Pardo, L.; Morales, D.; Menendez, M. L. *Questiio* **1989**, *13*, 47.

(11) Kullback, S.; Leibler, A. *Ann. Math. Stat.* **1951**, *22*, 79.

(12) Antolin, J.; Angulo, J. C.; López-Rosa, S. *J. Chem. Phys.* **2009**, *130*, 074110.

(13) Lin, J. *IEEE Trans. Inf. Theory* **1991**, *37*, 145.

(14) Hoffman, R.; Shaik, S.; Hiberty, P. C. *Acc. Chem. Res.* **2003**, *36*, 750.

(15) Schlegel, H. B. *Adv. Chem. Phys.* **1987**, *67*, 249.

(16) Fukui, K. *Acc. Chem. Res.* **1981**, *14*, 363.

(17) Shaik, S.; Ioffe, A.; Reddy, A. C.; Pross, A. *J. Am. Chem. Soc.* **1994**, *116*, 262.

(18) Eyring, H. *J. Chem. Phys.* **1935**, *3*, 107. Wigner, E. *Trans. Faraday Soc.* **1938**, *34*, 29.

(19) Hammond, G. S. *J. Am. Chem. Soc.* **1955**, *77*, 334. Leffler, J. E. *Science* **1953**, *117*, 340.

(20) Shi, Z.; Boyd, R. J. *J. Am. Chem. Soc.* **1991**, *113*, 1072.

(21) Bader, R. F. W.; MacDougall, P. J. *J. Am. Chem. Soc.* **1985**, *107*, 6788. Balakrishnan, N.; Sathyamurthy, N. *Chem. Phys. Lett.* **1989**, *164*, 267. Ho, M.; Schmider, H. L.; Weaver, D. F.;

Smith, V. H., Jr.; Sagar, R. P.; Esquivel, R. O. *Int. J. Quantum Chem.* **2000**, *77*, 376. Knoerr, E. H.; Eberhart, M. E. *J. Phys. Chem. A* **2001**, *105*, 880. Tachibana, A. *J. Chem. Phys.* **2001**, *115*, 3497.

(22) Gadre, S. R. In *Reviews of Modern Quantum Chemistry: A Celebration of the Contributions of Robert G. Parr*; Sen, K. D., Ed.; World Scientific: Singapore, 2003; Vol. 1, pp 108−147. Koga, T.; Morita, M. *J. Chem. Phys.* **1983**, *79*, 1933. Ghosh, S. K.; Berkowitz, M.; Parr, R. G. *Proc. Natl. Acad. Sci. U.S.A.* **1984**, *81*, 8028. Angulo, J. C.; Dehesa, J. S. *J. Chem. Phys.* **1992**, *97*, 6485. Massen, S. E.; Panos, C. P. *Phys. Lett. A* **1998**, *246*, 530. Nalewajski, R. F.; Parr, R. G. *J. Phys. Chem. A* **2001**, *105*, 7391. Nagy, A. *J. Chem. Phys.* **2003**, *119*, 9401. Romera, E.; Dehesa, J. S. *J. Chem. Phys.* **2004**, *120*, 8906. Karafiloglou, P.; Panos, C. P. *Chem. Phys. Lett.* **2004**, *389*, 400. Sen, K. D. *J. Chem. Phys.* **2005**, *123*, 074110. Parr, R. G.; Nalewajski, R. F.; Ayers, P. W. *J. Phys. Chem. A* **2005**, *109*, 3957. Guevara, N. L.; Sagar, R. P.; Esquivel, R. O. *J. Chem. Phys.* **2005**, *122*, 084101. Shi, Q.; Kais, S. *J. Chem. Phys.* **2005**, *309*, 127. Chatzisavvas, K. Ch.; Moustakidis, Ch. C.; Panos, C. P. *J. Chem. Phys.* **2005**, *123*, 174111. Sen, K. D.; Katriel, J. *J. Chem. Phys.* **2006**, *125*, 074117. Nagy, A. *Chem. Phys. Lett.* **2006**, *425*, 154. Ayers, P. W. *Theor. Chem. Acc.* **2006**, *115*, 253. Martyusheva, L. M.; Seleznev, V. D. *Phys. Rep.* **2006**, *426*, 1. Liu, S. *J. Chem. Phys.* **2007**, *126*, 191107. Borgoo, A.; Jaque, P.; Toro-Labbé, A.; Van Alsenoy, Ch.; Geerlings, P. *Phys. Chem. Chem. Phys.* **2009**, *11*, 476.

(23) Esquivel, R. O.; Flores-Gallegos, N.; Iuga, C.; Carrera, E.; Angulo, J. C.; Antolin, J. *Theor. Chem. Acc.* **2009**, *124*, 445–460.

(24) Rawlings, D. C.; Davison, E. R. *J. Phys. Chem.* **1985**, *89*, 969.

(25) Kaijser, P.; Smith, V. H., Jr. *Adv. Quantum Chem.* **1997**, *10*, 37.

(26) Kohout, M. *Program DGRID, version 4.2*; 2007.

(27) Hamilton, I. P.; Mosna, R. A. *J. Comput. Appl. Math.* **2010**, *233*, 1542–1547.

(28) Dehesa, J. S.; Gonzalez-Ferez, R.; Sanchez-Moreno, P. *J. Phys. A* **2007**, *40*, 1845.

(29) Politzer, P.; Truhlar, D. G. *Chemical Applications of Atomic and Molecular Electrostatic Potentials*; Academic Press: New York, 1981.

(30) Parr, R. G.; Pearson, R. G. *J. Am. Chem. Soc.* **1983**, *105*, 7512. Parr, R. G.; Yang, W. *Density-Functional Theory of Atoms and Molecules*; Oxford University Press: New York, 1989. Geerlings, P.; De Proft, F.; Langenaeker, W. *Chem. Rev.* **2003**, *103*, 1793.

(31) Koopmans, T. *Physica A* **1933**, *1*, 104. Janak, J. F. *Phys. Rev. B* **1978**, *18*, 7165.

(32) Ghanty, T. K.; Ghosh, S. K. *J. Phys. Chem.* **1993**, *97*, 4951. Roy, R.; Chandra, A. K.; Pal, S. *J. Phys. Chem.* **1994**, *98*, 10447. Hati, S.; Datta, D. *J. Phys. Chem.* **1994**, *98*, 10451. Simon-Manso, Y.; Fuenteaelba, P. *J. Phys. Chem. A* **1998**, *102*, 2029.

(33) Chattaraj, P. K.; Sarkar, U.; Roy, D. R. *Chem. Rev.* **2006**, *106*, 2065.

(34) Pearson, R. G. *J. Am. Chem. Soc.* **1963**, *85*, 3533. Pearson, R. G. *Hard and Soft Acids and Bases*; Dowen, Hutchinson and Ross: Stroudsberg, 1973. Pearson, R. G. *Chemical Hardness*; Wiley-VCH: New York, 1997.

(35) Frisch, M. J.; Trucks, G. W.; Schlegel, H. B.; Scuseria, G. E.; Robb, M. A.; Cheeseman, J. R.; Montgomery, J. A., Jr.; Vreven, T.; Kudin, K. N.; Burant, J. C.; Millam, J. M.; Iyengar, S. S.; Tomasi, J.; Barone, V.; Mennucci, B.; Cossi, M.; Scalmani, G.; Rega, N.; Petersson, G. A.; Nakatsuji, H.; Hada, M.; Ehara, M.; Toyota, K.; Fukuda, R.; Hasegawa, J.; Ishida, M.; Nakajima, T.; Honda, Y.; Kitao, O.; Nakai, H.; Klene, M.; Li, X.; Knox, J. E.; Hratchian, H. P.; Cross, J. B.; Bakken, V.; Adamo, C.; Jaramillo, J.; Gomperts, R.; Stratmann, R. E.; Yazyev, O.; Austin, A. J.; Cammi, R.; Pomelli, C.; Ochterski, J. W.; Ayala, P. Y.; Morokuma, K.; Voth, G. A.; Salvador, P.; Dannenberg, J. J.; Zakrzewski, V. G.; Dapprich, S.; Daniels, A. D.; Strain, M. C.; Farkas, O.; Malick, D. K.; Rabuck, A. D.; Raghavachari, K.; Foresman, J. B.; Ortiz, J. V.; Cui, Q.; Baboul, A. G.; Clifford, S.; Cioslowski, J.; Stefanov, B. B.; Liu, G.; Liashenko, A.; Piskorz, P.; Komaromi, I.; Martin, R. L.; Fox, D. J.; Keith, T.; Al-Laham, M. A.; Peng, C. Y.; Nanayakkara, A.; Challacombe, M.; Gill, P. M. W.; Johnson, B.; Chen, W.; Wong, M. W.; Gonzalez, C.; Pople, J. A. *Gaussian 03*, revision D.01; Gaussian, Inc.: Wallingford, CT, 2004.

(36) Johnson, B. A.; Gonzales, C. A.; Gill, P. M. W.; Pople, J. A. *Chem. Phys. Lett.* **1994**, *221*, 100.

(37) Shi, Z.; Boyd, R. J. *J. Am. Chem. Soc.* **1989**, *111*, 1575.

(38) Pérez-Jordá, J. M.; San-Fabián, E. *Comput. Phys. Commun.* **1993**, *77*, 46. Pérez-Jordá, J. M.; Becke, A. D.; San-Fabián, E. *J. Chem. Phys.* **1994**, *100*, 6520.

(39) Schaftenaar, G.; Noordik, J. H. *J. Comput.-Aided Mol. Des.* **2000**, *14*, 123.

(40) Toro-Labbé, A.; GutiÃl'rrez-Oliva, S.; Murray, J. S.; Politzer, P. J. *Mol. Model.* **2009**, *15*, 707. Toro-Labbé, A.; GutiÃl'rrez-Oliva, S.; Murray, J. S.; Politzer, P. *Mol. Phys.* **2007**, *105*, 2619. Murray, J. S.; Toro-Labbé, A.; Clark, T.; Politzer, P. J. *Mol. Model.* **2009**, *15*, 701. Jaque, P.; Toro-Labbé, A.; Geerlings, P.; De Proft, F. *J. Phys. Chem. A* **2009**, *113*, 332.

(41) Glukhovtsev, M. N.; Pross, A.; Radom, L. *J. Am. Chem. Soc.* **1995**, *117*, 2024.

(42) Polanyi, J. C.; Zewail, A. H. *Acc. Chem. Res.* **1995**, *28*, 119.

CT900544M